Peer-reviewed version available at *Magnetochemistry* **2018**, *4*, 36; doi:10.3390/magnetochemistry4030036

Overview on Induced Chirality in Magnetic Field Controlled Electro-Deposition and Induced Magnetic Moment Originating from Chiral Electrodes

Anup Kumar[†], Prakash Chandra Mondal[§] and Claudio Fontanesi[‡]*

[†]Department of Chemical and Biological Physics, Weizmann Institute of Science, Rehovot 76100, Israel.

[§] Institute of Molecular Science (ICMOL), University of Valencia, Paterna 46980, Spain

[‡]DIEF, University of Modena and Reggio Emilia, Via Vivarelli 10, Modena 41125, Italy

Abstract

Magneto-electrochemistry (MEC) is a unique paradigm in science, where electrochemical experiments are carried out as a function of an applied magnetic field, creating a new horizon of potential scientific and technological applications. Over the time, detailed understanding of this research domain was developed to identify and rationalize the possible effects exerted by a magnetic field on the various microscopic processes occurring in an electrochemical system, such as: electrolyte properties governed by charge-transfer process (electric conductivity, viscosity, and diffusivity), mass transfer, electrochemical kinetics and on the structure/quality of products formed either at the working electrode or in the electrochemical cell. Particularly, magnetic field controlled chiral architecture obtained from deposited metal, alloys and catalyst and their excellent enantio-recognition in experimental frame is highly appealing. Interestingly, Hall effect was also demonstrated in electrolytic medium via an impressive experimental technique which is being employed for further theoretical understanding in the field of magneto-electrochemical science. Later, a highly reproducible local temperature variation was observed in electrochemical electrolytes exposed to perpendicular magnetic and electric fields. However, until recent studies, none of the above mentioned reports considered the possibility of a spin-dependent related charge-transfer process. Recent experimental and theoretical studies reveal that electron's transmission through chiral molecules is spin-selective and this effect has been referred to as chiral-induced spin-selectivity (CISS) effect. The CISS effect pave the way for the building up of a system characterized by a net magnetic moment exploiting the spin-filtering ability of chiral molecules. This interplay between chirality and magnetism may shed light on fundamental scientific aspects underlying the enantio-recognition and highly efficient electron-transfer that occurs in biological process.

E-mail: claudio.fontanesi@unimore.it

Keywords: Magnetoelectrochemistry; CISS; spin; chirality; spin-dependent electrochemistry

Peer-reviewed version available at Magnetochemistry 2018, 4, 36; doi:10.3390/magnetochemistry4030036

1. Introduction

Magneto-electrochemistry (MEC) combines two distinct paradigm i.e., electrochemistry and magnetism where surprising outcomes are possible on changing direction of superimposition of two variables causing complex hydrodynamics response from the electrolyte and redox ions [1]. Indeed, the influence of the magnetic field on electrochemical process, in a variety of ways and experimental configurations, has been first observed by Michael Faraday [2].

A number of parallel attempts were made to elucidate the effect of a magnetic field on the electrolyte properties, mass transfer, electrochemical kinetics and the structure/morphology and quality of the electrodeposited films [3]. One of the most interesting and persistent observation was the chiral texture of electrodeposited films, such as metals (Cu, Ag, Fe *etc*), alloys, conducting polymers (polyaniline, *etc*), such modified morphology is useful in advanced applications like enantioselective recognition/adsorption processes [4].

So far most of the studies in the literature used an external magnetic field to generate chiral potential. Of late, Naaman et. al., discovered a revolutionary "chiral induced spin selectivity (CISS)" effect, which states that transport of electrons through chiral molecules depends on their spin states and give rise to a net magnetic moment (with the associated magnetic field) [5], and references therein cited. The idea was recently demonstrated via an innovative Hall device that serves as the working electrode in an electrochemical cell, and is capable of providing information on the correlation of spin selectivity and the electrochemical process without an external field[6].

Thus, our intent here is to give a brief overview of the recent experimental findings obtained by combining magneto-electrochemical systems and chiral architectures, like in 2D metallic or organic electrodeposition under an external imposed magnetic field and their enantioselective recognition/adsorption processes [7]. In addition, the second part of this review highlights the exciting results obtained by spin-specific electron transmission through chiral interfaces in electrochemical systems.

2. Magnetic effect on the electrolyte solution

2.1. Lorentz force on electrolytic solution.

Peer-reviewed version available at Magnetochemistry 2018, 4, 36; doi:10.3390/magnetochemistry4030036

The electrolytic solution provides a conductive medium for the movement of ions under an applied electric field E, and the electrostatic force exerted on moving ions carrying charge q is given by the relation [8]:

$$F = qE, \quad (1)$$

Application of a uniform magnetic field B, together with the electric field on the conductive ion would subject a Lorentz type force expressed by the equation [9]:

$$F = q(E + v \times B), \quad (2)$$

where v is the velocity of the ion. Equation (2) gives due reason to the deviation from the linear trajectory as previously shown in Hall effect in semiconductor [10]. This is referred to as the magneto-hydrodynamics (MHD) force and for this discovery the Nobel Prize was awarded to Hannes Alfven in 1970 [11]. Moreover, the effect of a uniform magnetic field on a conductive fluid in electrochemical cell is different from those of a magnetic field gradient in simple electrostatics. The influence of non-uniform magnetic field is quantitatively evaluated as follows:

$$\vec{F}_{mag} = \frac{\chi_m B^2 \vec{\nabla} c}{2\mu_0} + \frac{\chi_m c_0 B \vec{\nabla} B}{\mu_0} \quad (3)$$

In relation (3) χ_m is the molar susceptibility, $\mu_0 = 4\pi \times 10^{-7}$ is the permeability of free space and c_0 is the bulk concentration of magnetic species in solution (mol/m^3). This expression of F_{mag} consists of two terms, the first term is the paramagnetic gradient force (which depends on the concentration gradient), the second term is the field gradient force (which can be significant whenever there is a non-uniform magnetic field, such as the surface of a rough ferromagnetic electrode).

2.2. Conductivity of solution under magnetic field

To account for the effect of a magnetic field on the electrical conductivity of an electrolyte is a rather complex task. Experimental results demonstrate that electrical conductivity increases by a factor of 1.04 – 1.2 at increasing the magnetic field intensity [2]. Tronel-Peyroz and Olivier [12] using a method analogous to the kinetic gas theory, studied the transport coefficient in an

electrolyte, under steady state conditions, in the presence of superimposed electric and magnetic fields. They have shown that the ionic mobility and the diffusion coefficients become tensor quantities, which depend on the magnetic field. The matrix that represents the ionic mobility of the species is:

$$\bar{u} = \begin{pmatrix} u_T & u_H & 0 \\ -u_H & u_T & 0 \\ 0 & 0 & u_{\|} \end{pmatrix}, \tag{4}$$

where u_T is the transverse mobility, u_H is the Hall mobility, $u_{\|} = u$ is the conventional mobility in the absence of the magnetic field. The matrix of diffusion can be deduced from the mobility by the following relation:

$$\bar{D} = \frac{KT}{q}\bar{u}, \tag{5}$$

Experimentally, in the case of ferro-ferrcyanide solutions in KCl, for a magnetic strength of about 1T on neglecting the diffusion term, the current induced by the field is given by:

$$J = \sigma(E + \mu\Gamma \times B) \tag{6}$$

Szcześ et. al., did an extensive study on effect of static magnetic field on water as a function of time [13]. The water conductivity was measured as a function of time following the application of magnetic field. It was demonstrated that the magnetic field decreases the water conductivity. The effects are due to the hydrogen bond network strengthening and the perturbation of gas/liquid interface from the air nano-bubbles in the water. Szcześ et. al. showed that for magnetized samples a decrease in the conductivity relative to non-magnetized sample appears, conductivity measurements with 15 mT magnetic field for 5 minutes shows significant enhancement in conductivity of water, this effect is found lasting for about 24 h. Thus suggesting some sort of a "memory effect" in water. However, memory of magnetic treatment was reported up to 200 h [14].

Kovarsky et. al. presented a procedure for orienting the polyethylene-oxide (PEO) helices in a direction perpendicular to the film plane by casting the polymer electrolytes (PE) under a static magnetic field of 1.22T [15]. The influence of varying the magnetic field intensity and orientation on the structural properties, and ionic conductivity as well, of concentrated lithium trifluoromethanesulfonate ($LiCF_3SO_3$) and $LiAsF_6$:P(EO) pristine and composite polymer

electrolytes containing γ-Fe_2O_3 nanoparticles was thoroughly studied. It was found that the higher the content of the crystalline phase and the size of spherulites in the typically cast salt-polymer system the stronger the influence of the magnetic field on the conductivity enhancement, when the electrolyte is casted and dried under magnetic field. For instance, $LiAsF_6$:$(PEO)_3$ at 65◦C exhibits a inter-chain conductivity rise by a factor of 75, while the intra-chain conductivity is increased by a factor of 11–14.

2.3. Diffusivity of electrolyte

Very few studies are available devoted to the influence of the magnetic field on diffusivity of solution and most of them reports relatively chemical species dependent effect.

2.4. Viscosity, temperature

The viscosity measured under magnetic field of 1T decreases with the increase of chemical species concentration. Thermal effects have been studied by Tronel-Peyroz and Olivier [16]. A local variation in the temperature has been observed when the electrolyte is subject to an electric and magnetic field perpendicular to each other, a topic discussed in more details in section 6.

3. Mass transport under magnetic field

Magnetic field effects on mass transport of electrolytes in electrochemical cell have been studied extensively. The magnetic field persuades convection in the electrolyte causing narrowing of the diffusion layer. It is experimentally shown that enhancement of up to 100% in limiting current is observed, the electrochemical current enhancement follows a $B^{1/3}c_0^{4/3}$ empirical law [17]. In the case of copper electro-deposition an exponential behavior of limiting current with applied magnetic field was observed. Aogaki et. al. proposed a semi-empirical model in good agreement with experimental data obtained for a channel electrode cell and validates the $B^{1/3}c^{4/3}$ behaviour of conducting electrolytes under magnetic field [18]. Moreover, exceeding a critical value of $jB > 950\ Nm^{-3}$ induces an interesting hydrodynamic turbulence in the electrochemical cell. Magnetic field effects influencing corrosion processes have been studied [19]. Also autocatalytic reactions are inhibited by the magnetic field effect, as corrosion products diffuse more easily following the stronger local induced convection.

4. Electrode kinetics

The effect of a magnetic field on the kinetics of the electrode reaction is considered as most controversial so far. The magnetic field has no significant effect on the kinetics as evaluated on the basis of Tafel data [20] and as it is found in magneto-impedance experiments [21]. A few reports do support that exchange current density is blocked under high magnetic field [22]. However, several other factors such as vigorous agitation of the solution or the use of a rotating disk electrode can contribute to the indirect kinetic effects. The effect of magnetic field on the rate of recombination of radical pairs have been studied by several reports [23], which support that magnetic fields either enhance or impede the coherent oscillation of the radical pair between its singlet and triplet states. On the contrary, magnetic field could not significantly influence the rate of a heterogeneous electrochemical reaction, since the magnetic field energy is negligible compared to both the thermal energy and the electrostatic potential energy.

5. Texture and Surface morphology

Application of a magnetic field during the processes of electro-deposition of metals, alloys and electropolymerization reactions gives raise to complex texture and morphology, a subject of great interest for material scientists. Several electrodeposited materials was reported to show chiral texture either with clockwise or anticlockwise orientation, due to complex convective effects depending on the magnetic field orientation with respect to the electrode [24]. Mhíocháin et. al. showed zinc fractal form electrodeposition grown around a point cathode in a flat, horizontal electrochemical cell [25]. When the zinc is electrodeposited under an applied perpendicular magnetic field a chiral spiral structure is developed, which interestingly reverses the handedness on switching the field direction from upwards to downwards, compare Figure 1.

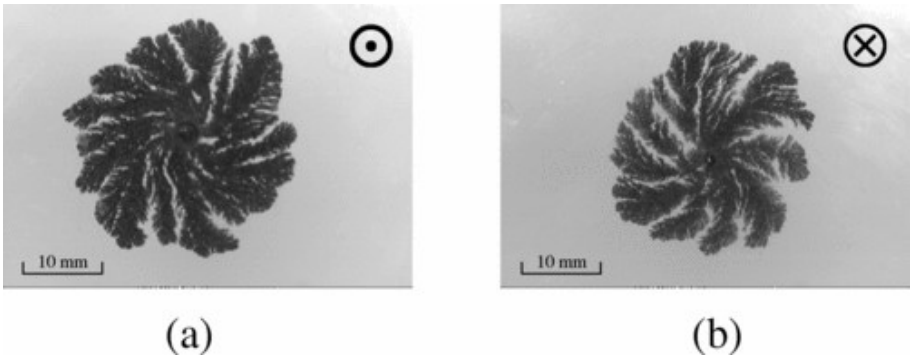

Figure 1. Magnetic field controlled zinc electrodeposition grown from 0.1 M $ZnSO_4$ at 10 V in a flat horizontal cell in the presence of a 0.35 T magnetic field applied (a) vertically upwards, and

(b) vertically downwards. Reprinted with permission from ref. [25]. Copyright 2004, The American Physical Society.

In addition, x-ray diffraction (XRD) and Scanning electron microscopy (SEM) analyses on nickel–iron alloys have highlighted modifications of the composition and the smoothness of the deposit grown under magnetic effect [26]. For cobalt–iron alloy, superimposition of the magnetic field leads to a change in texture orientation without any modification of the composition of the deposit [27]. Finally, also the electropolymerization of organic compounds shows a dependence on the presence of magnetic field; for instance chiral manifestations have been observed during polyaniline electro-polymerization under high magnetic fields [28]. Importantly, chiral surfaces can act as enantio-selective catalysts capable of separating two enantiomeric forms of a product [29] and to be built in a variety of ways such as by adsorbing chiral molecules [30] or slicing single crystals so that they exhibit high-index faces [31].

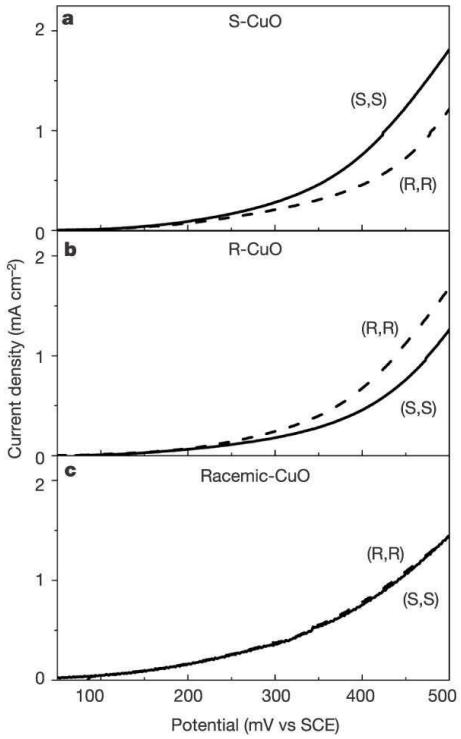

Figure 2. Enantio-recognition by electrodeposited chiral CuO. Electrocatalytic activity of (a) (S)-CuO, (b) (R)-CuO and (racemic)-CuO films towards oxidation of (R,R) and (S,S) tartaric acid. Reprinted with permission from ref. [32]. Copyright 2003, Nature Publishing Group.

Switzer et al. proposed a method to allow to producing a chiral surface of copper oxide through electro-deposition in the presence of chiral tartrate ion [32]. Interestingly, the chirality of the copper oxide surface can be tuned by changing the chirality of the tartrate ion in solution. In order to analyze the surface chirality, the electrochemical oxidation of uncomplexed (S,S)- and (R,R)-tartrate was determined. Figure 2a shows the oxidation of (S,S)- and (R,R)-tartrate on CuO electrodes that were deposited from Cu(II) (S,S)-tartrate and Cu(II) (R,R)-tartrate Figure. 2b. Notably, (S)-CuO film grown in (S,S)-tartrate is more active for the oxidation of the (S,S)-tartrate. On the contrary, (R)-CuO film is found active for (R,R)-tartrate. However, control film which was carried out on the racemic surface shows no selectivity for the oxidation of the any enantiomers Figure 2c. Importantly, CuO has been reported to be a potent electrocatalyst for the oxidation of carbohydrates, amino acids, simple alcohols, aliphatic diols, and alkyl polyethoxy alcohol detergents [33] and can open a pathway for high enantiomeric excess (ee) in chemical reaction.

Similarly, Hinds et. al., investigated the effect of a static magnetic field on the electrolysis of copper in aqueous solution and observed significant enhancement of the electro-deposition rate (up to 300%) from concentrated $CuSO_4$ solution at low pH [34]. Moreover, in this study, it was found that effect of the magnetic field is equivalent to the response obtained by using a rotating electrode. The magnetic field effect on the voltammogram (in the +2 to -2 V potential range, at the scan rate of 10 mV/s) recorded on a copper working electrode (0.75 M $CuSO_4$ solution at pH ~ 0.5) was studied. The scan consists of three distinct regimes namely: the activation regime close to the rest potential and the mass transport regime (current plateau) and hydrogen evolution regime (cathodic branch below -800 mV). No effect of the field is evident in the activation regime. Hydrogen evolution regime indicates suppression under higher fields. Importantly in mass transport regime, the current density at -500mV in the cathodic scan increases by a factor of 4 applying a magnetic field: from 1300 A/m^2 in zero field to 5400 A/m^2 in a field of 6 T. The anodic currents density is 2-3 times smaller than cathodic density and identical behavior of enhancement in the current density was observed i.e., current density at +1.5 V is increased from 600 A/m^2 in zero field to 1900 A/m^2 in a magnetic field of 6 T. The effect is independent of field direction and saturates at field larger than 6 T. Induced convective flow is affected by the magnetic field on a microscopic scale in the boundary layer close to the working electrode, thus altogether gravitational and magnetic force governs the morphology and fractal dimensionality.

Experiments were also performed to study the morphology of fractal electrodeposited films grown in the flat circular cells, in a horizontal orientation from a 0.2 M $CuSO_4$ solution at an applied voltage of 6V as a function of magnetic field intensity and orientation.

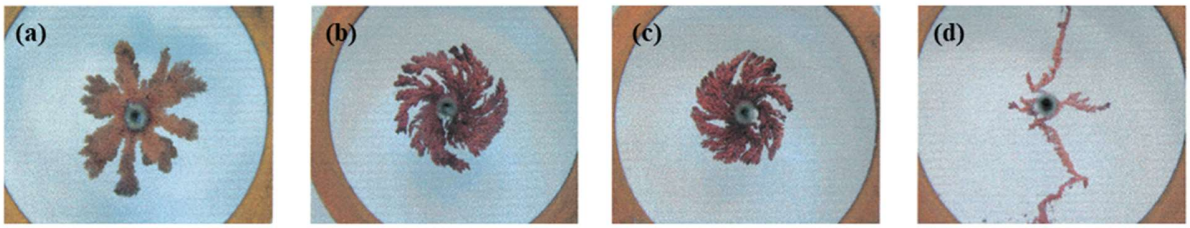

Figure 3. Morphology of copper electrodeposits grown around a central cathode in a horizontal flat circular cell (a) in zero applied field, (b) 0.4 T vertically upward (c) 0.4 T vertically downward, and (d) 1 T horizontally. Reprinted with permission from ref. [34]. Copyright 2001, American Chemical Society.

Dense radial growth is obtained in the absence of an applied magnetic field, Figure 3a, when a magnetic field is applied perpendicular to the plane of the cell, a branched chiral spiral-pattern forms Figure 3b, which reverses handedness with flipping the field direction Figure 3c. While parallel magnetic field to the plane of the cell, produces a stringy asymmetrical deposit, Figure 3d, predominatly in the direction where the Lorentz force and the gravitational force both act downward.

Similarly, chiral conducting polymer i.e., polyaniline doped with (+) - or (−)-camphor-10-sulfonate (CSA−) recognized the L- and D-ascorbic acid (AA) results different interaction as probed by electrical current measurements [28]. The latter results manifested chiral probing in current as L-AA shows a larger current than D-AA on the chiral electrode prepared from (−)-CSA−-doped polyaniline, and D-AA shows a larger peak current than L-AA on the opposite handedness electrode. These results indicate that the helical polyaniline film possess the ability of chiral recognition for L- and D-AA.

Yutthalekha et. al. describe the mesoporous metal structures with encoded geometric chiral information for inducing asymmetry in the electrochemical synthesis of mandelic acid as a model molecule [35]. The chiral-encoded mesoporous metal, obtained by the electrochemical reduction of platinum salts in the presence of a liquid crystal phase and the chiral template molecule, perfectly retains the chiral information after removal of the template. Significant enantiomeric excess of the (R)-enantiomer when using (R)-imprinted electrodes and vice versa

for the (S)-imprinted ones was successfully demonstrated. Moreover, changing the polarity of chiral cavities in the material allows tuning of enantio-selectivity.

6. Hall effect in electrolyte

The observation of Hall voltage in electrolytic solution is considered to be quite controversial when first shown by Roiti way back in 1882 yet with dedicated efforts of Frank and Hoffman [36]. The first successful evidence of Hall voltage in electrolyte solution was reported in 1975. Positive Hall coefficient for $CuSO_4$ liquid electrolyte has been measured which depends on polarity and strength of current and magnetic field, compare Figure 4. The Hall coefficient increases with decreasing the concentration of solute and show H^+ ion as major charge carrier in a liquid electrolyte with the carrier mobility of the order of 1 cm^2/volts-sec.

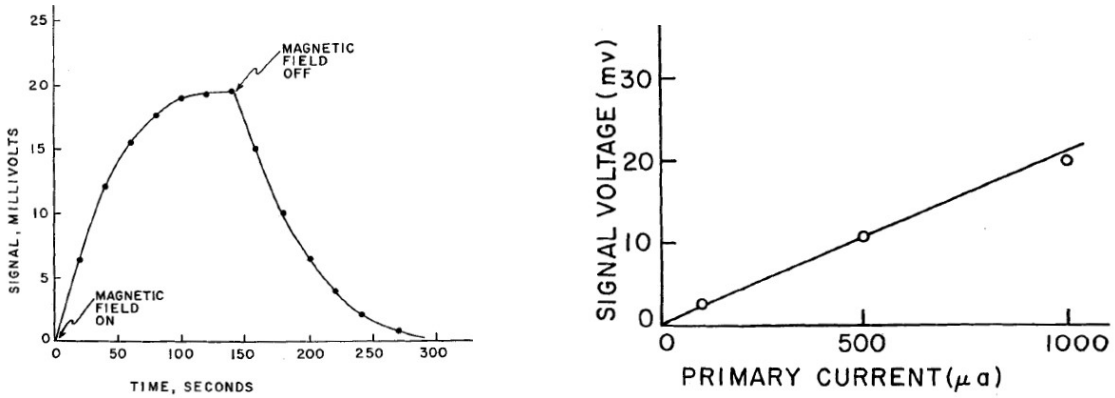

Figure 4. (a) Hall voltage developed on the application of magnetic field in 0.01 molar copper sulfate solution in water in time domain (sec). (b) Hall voltage (mV) obtained in 0.01 M $CuSO_4$ as a function of primary current (μA) in the solution. Reprinted with permission from ref. [36]. Copyright 1972, Taylor & Francis.

After this report, Hubbard and Wolynes theoretically calculated the electrohydrodynamic forces on an ion moving in a polarizable liquid in a magnetic field [37]. The result is a hydrodynamic force which is about 30% of the Lorentz force q/c (v x B). The calculation indicated that the effect is independent of ion size, charge and solvent viscosity. Moreover, Newman et. al, exploited the solid electrolyte $C_5H_6NAg_5I_6$ for demonstrating the Hall effect [38]. The ionic Hall effect was measured in the order of 10-100 nV at 25°C for 0.1-1.0 T, respectively. The exceptionally high ionic conductivity in $C_5H_6NAg_5I_6$ at 25°C is assigned to a relatively small number of mobile Ag^+ ions. Hall effect in electrolyte was considered as spurious due to local variations of salt concentration. Interestingly, Wright and Van der Beken showed significant Hall

Peer-reviewed version available at Magnetochemistry 2018, 4, 36; doi:10.3390/magnetochemistry4030036

voltage in flowing electrolyte under the magnetic field with the flow-velocity of electrolyte [39]. They observed that a charged particle moving through a magnetic field experiences a force qv x B, causing separation of positive and negative ions by the Lorentz force and produce an electric field generating linearly increasing hall voltage across the flow tube with the flow rate.

6. Temperature variation in magnetic field

Notably, a minor but highly reproducible temperature rise was observed when a DC current was passed through an electrolytic cell placed in a uniform constant magnetic field, whose magnitude can be a fraction of a degree, remain symmetrical as the direction of the current is alternated upon reaching steady state. Tronel-Peyroz and Olivier demonstrated the variation of such temperature differences with current (at a fixed value of B), which is an initial decrease, followed by a monotonic increase after the achieving of a minimum value [16]. Olivier models the temperature variations in terms of the kinetic energy of ions and the ionic relaxation time on the basis of Boltzmann's classical distribution equations and ascribed to slight changes in the degree to the dissociation of water caused by the magnetic field. Accurate estimation of heats of ion transfer in magnetic fields might be one useful application of this methodology.

7. Induced magnetic field via chiral molecules

7.1. 3D electrochemistry using chiral molecules

“Three-dimensional (3D) spin-electrochemistry” methodology is based on Hall potential measurements performed in an electrochemical systems: the spin-filtering due to the chiral electrode interface leads to spin accumulation, resulting in a magnetic field [40]. This method provides simultaneously, in operando, a three-way source of information about the applied voltage, the resulting electrochemical current, and spin injection/magnetic moment which is probed via the Hall potential measurements. This device is based on the use of a AlGaN/GaN high electron mobility transistor (HEMT) [41]. This device serves two purposes: it is the working electrode as in a conventional electrochemical cell and, simultaneously, it measures the spin polarization of the current, as presented schematically in Figure 5. CV measurements are expedient to force a current flow at the chiral electrode interface (made chiral by adsorption of a polypetide monolayer). Spin accumulation in the HEMT device originates a relevant magnetic field which is detected by measuring the Hall potential in the channel where a constant current is

pumped between the source and drain electrodes (S and D in Figure 5a) [42]. The Hall potential stems from the spin-polarized electrons injected into (or out from) the GaN device. The accumulated spins in the GaN produce a magnetic field perpendicular to the modified working electrode device's surface.

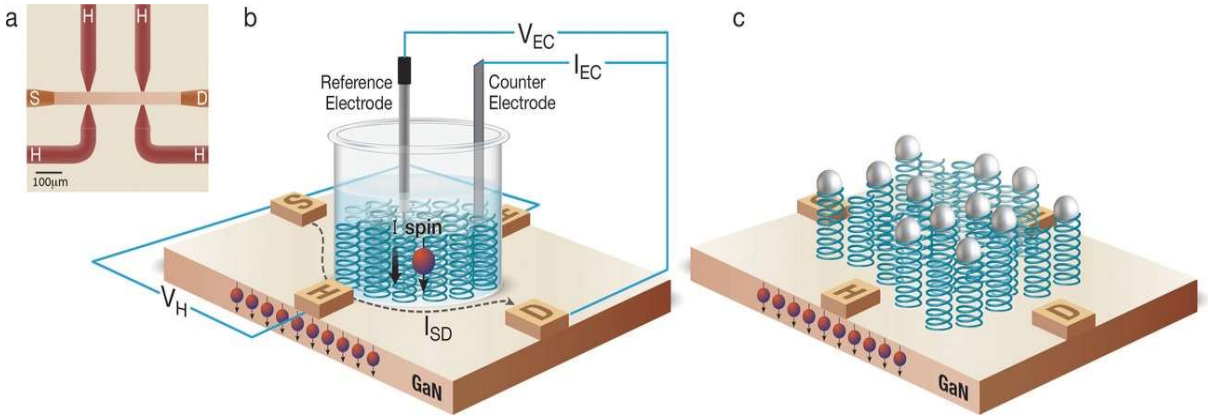

Figure 5: A scheme of the experimental set-up: (a) Optical microscope image of the GaN based Hall device. S and D are the source and drain electrodes, respectively, and H denotes the electrodes used for Hall measurements. (b) The pictorial view of combined electrochemical/Hall device apparatus. (c) Working electrode with silver nanoparticles (AgNPs) as the redox probe attached to the adsorbed oligopeptides. Reprinted with permission from ref. [42]. Copyright 2017, WILEY-VCH.

This method generates the magnetic field via spin filtering obtained by charge transmission through the chiral interface, via CISS effect. This is important since it is known that magnetic fields introduce various effects, as discussed in previous sections, that may influence the global electrochemical behavior of a system, even if there is no spin-dependent reaction [9].

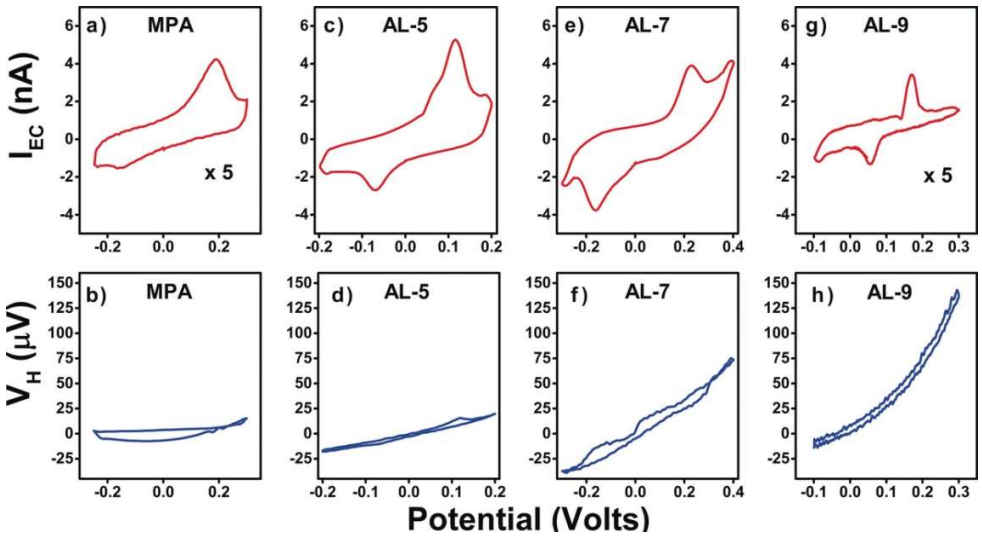

Figure 6. Electrochemical and Hall potential measurements results obtained when the GaN device is coated with a self- assembled monolayers of achiral molecules (MPA: 3-mercapto propanoic acid) or with chiral α-helical oligopeptides of variable length L-SH-CH_2-CH_2-CO-{Ala-Aib}$_n$-COOH, where n = 5, 7, and 9 for AL-5, AL-7, and AL-9, respectively. Reprinted with permission from ref. [42]. Copyright 2017, WILEY-VCH.

This method probes the spin selectivity of electrons transmitted through a monolayer of chiral molecules of various lengths. The α-helical oligopeptides are covalently bound to the surface via the carboxylic group (C-terminal) and to silver clusters (15-20 nm in diameter) acting as the redox probe. Remarkably, the current in the cyclic voltammograms is almost identical for all the four adsorbed molecules, while the relevant Hall potential difference increases with the length of the adsorbed molecules. This is due to continuous injection of spin polarized electrons from the solution to the GaN electrode, compare Figure 6. This method allows to obtain a relatively long lifetime of the spins within GaN, then polarized spins are accumulated yielding a measurable magnetic field.

Preprints (www.preprints.org) | NOT PEER-REVIEWED | Posted: 12 June 2018 doi:10.20944/preprints201806.0186.v1

Peer-reviewed version available at Magnetochemistry 2018, 4, 36; doi:10.3390/magnetochemistry4030036

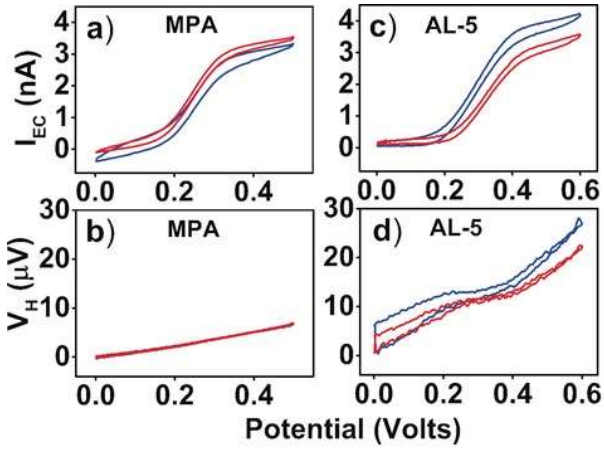

Figure 7: The enantio-selectivity data for devices coated with achiral molecules (a,b) and with chiral AL-5 (c,d) with R-and S-ferrocene (blue and red curves, respectively). Reprinted with permission from ref. [42]. Copyright 2017, WILEY-VCH.

Chiral GaN-based working electrode is applied for conducting an enantio-specific electrochemical process to validate the correlation between enantio-selectivity with the spin polarization [6]. The device was coated with AL-5 and similar experiment as described above is performed with chiral redox couple either (S)-(-)-N,N-Dimethyl-1-ferrocenylethylamine or (R)-(+)-N,N-Dimethyl-1-ferrocenylethylamine (S and R ferrocene, respectively) dissolved in phosphate buffer (pH ~ 7). Since the device has a small surface area 20×10^3 μm^2 , it is not expected to observe the redox peaks in this type of experiments [43]. Owing to the chiral working electrode, we observed enhanced current in the CV curve with R-ferrocene, as shown in Figure 7c with higher Hall potential for favorable spin-interaction Figure 7d while no significant effect is visible in achiral analogues device Figure 7b.

7.2. Magnetic field using electrolytic gated chiral molecules

Kumar et. al. demonstrated experimentally that, in chiral molecules, charge redistribution is accompanied by spin polarization [6]. The spin polarization was measured by using a Hall-effect device similar to that described in section 7.1. An electric field that is applied along the molecules causes charge redistribution, and for chiral molecules, a Hall voltage is measured that indicates the spin polarization/magnetic field on the surface. During this experiment, a Hall device, coated with a self-assembled organic monolayer, is placed in solution with a gate electrode (G) electrode, not in direct contact with the solution, and an inert electrolyte. When an electric potential V_G is applied between the G electrode and the device, the ionic solution is

polarized, so that an electric field acts on the adsorbed molecules in Figure 8A. The relevant electrical scheme is shown in Figure 8B: I_{SD} indicates the applied S–D current, V_G is the gate voltage, and V_H is the differential Hall potential across the conductive channel.. As a result, the molecules are polarized because of charge reorganization (partial charges q+ and q−), inducing a charge displacement in the surface region of the device. Because the charge polarization is accompanied by spin polarization (red balls with black arrows, compare Figure 8C), a magnetic field that acts on the electrons flowing between the S and D electrodes is also created. It is important to realize that the ability to observe a significant Hall potential results, in part, from the proximity of the polarized spin distribution to the conductive channel. The Hall potential V_H, which is formed as a result of the spin magnetization, was measured as a function of V_G.

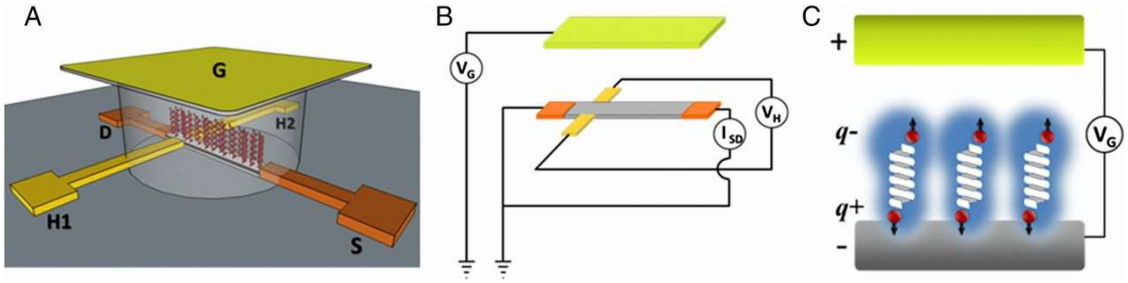

Figure 8. (A) The pictorial view of experimental set-up, (B) electrical connections and (C) concept behind of the Hall potential measurements. Reprinted with permission from ref. [6]. Copyright 2017, United States National Academy of Sciences (United States).

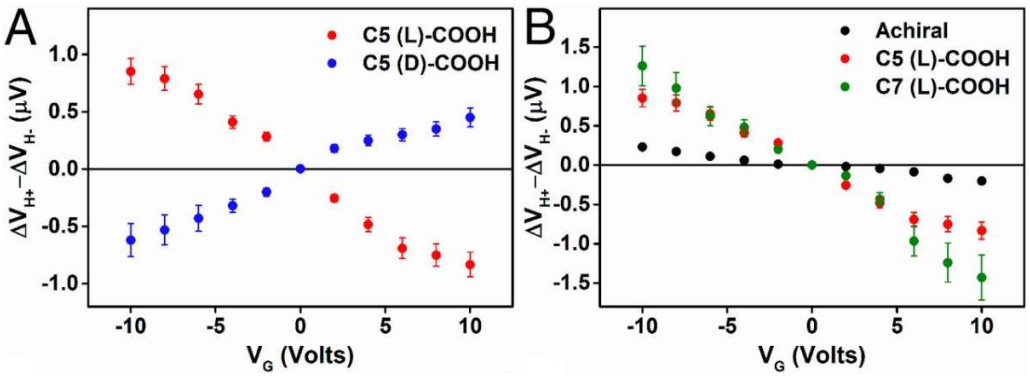

Figure 9. Hall measurements conducted on devices coated with different oligopeptides. (A) Hall potential measured when the adsorbed layer is either L-SH-CH_2-CH_2-CO-{Ala-Aib}$_5$-COOH (red) or D-SH-CH_2-CH_2-CO-{Ala-Aib}5-COOH (blue). (B) The dependence of the Hall voltage on V_G is shown for monolayer films of achiral 11-mercapto-undecanoic acid (black), chiral L-SH-CH_2-CH_2-CO-{Ala-Aib}$_5$-COOH (red), and chiral L-SH-CH_2-CH_2-CO-{Ala-Aib}$_7$-COOH (green). Reprinted with permission from ref. [6]. Copyright 2017, United States National Academy of Sciences (United States).

Figure 9A shows the Hall voltages as a function of the gate potential for the chiral oligopeptides: L- and D-SH-CH_2-CH_2-CO-{Ala-2-aminoisobutyric acid or 2-methylalanine (Aib)}$_5$-COOH where L and D refer to the different handedness of the amino acid units. The Hall voltage observed with the chiral molecules shows a nearly linear dependence on the applied gate voltage, and its sign depends on the chirality of the molecule. Figure 9B sets out Hall potential V_H data measured for two chiral L-oligopeptides of different length and an achiral molecule as a control. Because of the high ordered molecular chirality with L-SHCH2CH2CO-{Ala-Aib}$_7$-COOH, higher spin polarization (possesses a magnetization) is created, which is responsible for the higher Hall voltage. Note that the intrinsic spin depolarization in GaN (which makes up the Hall device) occurs on a submicrosecond timescale, the high capacitance of the measurement leads to a signal that decays with the time constant of the system (1/RC, where R is the total resistance (device and electrolyte solution) and C is the ionic capacitance . It is important to appreciate that, because of the high capacitance of the device, the measure signal is broadened in time, and therefore, the actual signal peak could be much larger. The device was calibrated using an external magnetic field. For an external voltage of 10 V, the Hall signal corresponds to about 5-mT field for the case of the SHCH2CH2CO-{Ala-Aib}$_7$-COOH. These results strongly suggest that effective magnetic field could be in turn, generated from the spin-filtering ability of the chiral adsorbed layer.

8. Spin-controlled charge-transport in chiral molecules

Spin-dependent charge-transport across chiral molecular assembly studied by spin-dependent electrochemistry is the first of its kind; specifically designed for measuring spin polarization (SP). Prof Naaman and his team established this state-of-the art technique in which chiral molecules can be deposited directly onto a ferromagnetic working electrode which can be magnetized either with its magnetic moment pointing “UP” or “DOWN” by placing a permanent magnet underneath the ferromagnetic electrode. The direction of the magnet can be flipped from “UP” to “DOWN” or vice-versa and simultaneously Faradic current can be measured under two different magnetized conditions by which spin polarization can be measured. Charge transmission through the chiral-electrode|solution interface is driven by an electrochemical charge-transfer process: a redox probe is suitably placed into an electrochemical cell, in bulk solution or immobilized on the electrode surface.

To study the spin-dependent electrochemical charge-transfer process, a ferromagnetic working electrode is used as a spin-injector [44]. High reactivity of the ferromagnetic electrodes requires special attention in order to minimize the oxide formation on the electrode surface [45]. Prof. Naaman and co-workers have established an adroit method to deposit molecules on metallic Ni electrode . For instance, freshly cleaned Ni was electrochemically reduced (-0.1 to -0.8 V vs SCE) and concurrently a monolayer of chiral polymer was grown over Ni working electrode. For instance, the chiral polymer, poly{[methyl N-(tert-butoxycarbonyl)-S-3-thienyl-L-cysteinate]-cothiophene} compare Figure 10a, of ~3 nm thickness was grafted and used for spin-dependent electrochemical study. An achiral ferrocene was introduced in an electrochemical cell and Faradic current was measured under spin "UP" and "DOWN" configurations, Figure 10b. The spin-dependent charge-transfer results are compelling as when the chiral polymer coated Ni electrode was magnetized "UP" direction, Faradic current changes its direction during oxidation to reduction process (red curve, Figure 10c). On the other hand, when the Ni working electrode was magnetized "DOWN" direction, cathodic current does not change its sign with reference to the anodic process. Thus "DOWN" spin-controlled electron-transfer process reveals a relatively higher energy barrier for electron conduction to occur from the nickel working electrode to the oxidized ferrocene molecules present in an electrolyte (black curve, Figure 10c). The same observation was made with the polymer-coated Ni electrode using chronoamperometric study. Thus a thin layer of chiral conductive polymer acts as an excellent spin filter, which allows the transmission of only one type of spin[46].

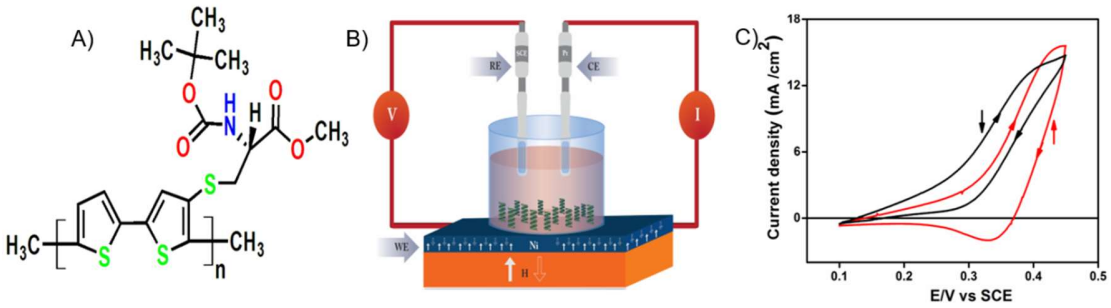

Figure 10: (A) Chemical structure of poly{[methyl N-(tert-butoxycarbonyl)-S-3-thienyl-L-cysteinate]- cothiophene}, (B) spin-dependent electrochemistry setup, where ferromagnetic Ni is coated with chiral polymers and used as the working electrode which can be magnetized by an external magnetic field (H), (C) spin-dependent cyclic voltammograms recorded on chiral polymer-coated Ni working electrode in presence of achiral ferrocene redox probe measured under magnetic field pointing "UP" (solid red curve), and "DOWN" (solid black curve) by

applying a static magnetic field of 0.35T. Reproduced with permission from ref. [46]. Copyright 2015 WILEY-VCH.

Biologically important macromolecules (such as oligopeptide, redox proteins which need nearly neutral pH ~7) can not be grown onto ferromagnetic electrode via in situ electrochemical reduction methods, because the high negative potential needed to reduce the nickel oxide may damage or denaturate its native forms. A recent study demonstrate an alternative way to prevent the oxide formation of the Ni electrode while allowing for the production of a surface suitable for Ni surface functionalization [47]. This result is obtained by growing a thin Au overlayer on top of the Ni substrate, without breaking the vacuum during the deposition process. Ni covered with an ultrathin Au overlayer is much more stable and was used to prepare self-assembled monolayers (SAMs) of L- and D-cysteine. The functional SAMs having free -NH_2 group was employed to make a covalent bond with an organic redox probe, toluidine blue O (TBO), compare Figure 11A, in order to measure Faradic current under an applied magnetic field of 0.35 T. Interestingly, two enantiomeric forms of TBO-Cys (L and D) showed opposite spin-polarization Figure 11B and C. D-Cys-TBO assembly shows spin-dependent Faradaic current and the spin polarization was measured at -6% for the oxidation peak potential at +0.185 V and +4.7% for the reduction process at -0.056 V SCE, Figure 11B. The L-Cys-TBO chiral assembly shows reverse spin polarization measured at +9% for oxidation process at 0.160 V, while the SP was at -7.5% found at reduction process at -0.024 V, Figure 11C. Spin-dependent cyclic voltammograms of L-Cys-TBO were recorded at increasing the Au overlayer thickness. Showing a neat decreases in spin-polarization upon increasing thickness of the gold overlayer on top of the Ni electrode.

Preprints (www.preprints.org) | NOT PEER-REVIEWED | Posted: 12 June 2018 doi:10.20944/preprints201806.0186.v1

Peer-reviewed version available at Magnetochemistry 2018, 4, 36; doi:10.3390/magnetochemistry4030036

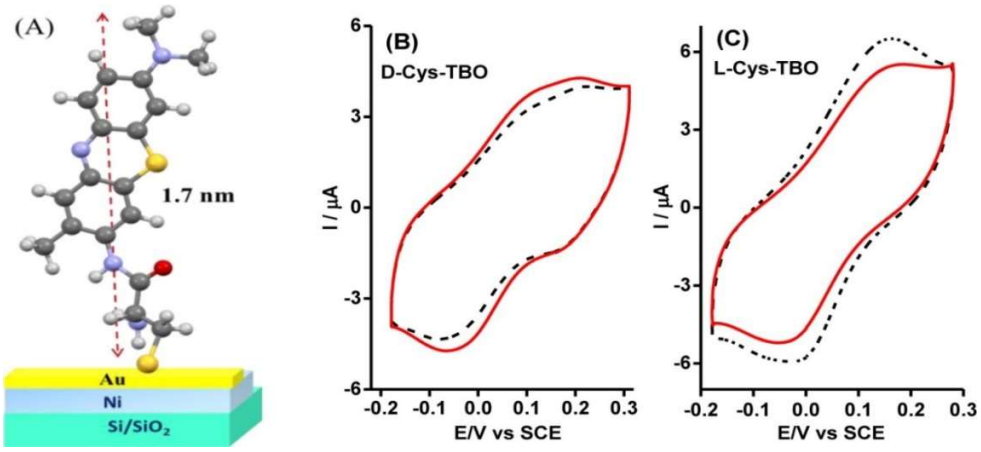

Figure 11: (A) Schematic description of covalently bonded toluidine blue O (TBO) to the SAMs of L or D cysteine prepared on 10 nm Au-coated Ni working electrode, (B) spin-dependent voltammograms of D-cys-TBO, and (C) L-cys-TBO assembly grafted on Au-overlayer coated Ni electrode. The voltammograms were recorded in 0.1 M PBS of pH 7.4 containing 10 mM KCl as supporting electrolyte at 50 mV s^{-1}. Reprinted with permission from ref. [47]. Copyright 2015 American Chemical Society.

9. Conclusions

This review focuses on the effect of magnetic field effects in different areas of electrochemistry. Electrodeposition and electropolymerization processes, electrolyte bulk charge transport and the quite recent spin-dependent electrochemistry are the topics here considered. In particular, spin-dependent electrochemistry, which is based on the interplay between chirality/spin/magnetic-field physical quantity, seems a promising approach for appealing applications in both sensor and adsorption related (chromatography) technological areas. Moreover, recent results show that chirality is able to drive spin-selective electron-transfer, through CISS effect, allowing to control local magnetic fields for highly advanced molecular based spintronic-devices.

Acknowledgements

PCM thanks European Union for Marie-Curie Fellowship (H2020-MSCA-2015-706238). C.F. acknowledges financial support for this research by University of Modena and Reggio Emilia (Department of Engineering 'Enzo Ferrari'), through "Spin Dependent Electrochemistry", FAR2016.

References

1. Coey, J. M. D.; Hinds, G. Magnetoelectrolysis - the effect of magnetic fields in electrochemistry. *Pamir* **2002**, 1–7.
2. Fahidy, T. Z. Magnetoelectrolysis. *J. Appl. Electrochem.* **1983**, *13*, 553–563, doi:10.1007/BF00617811.
3. Bund, A.; Koehler, S.; Kuehnlein, H. H.; Plieth, W. Magnetic field effects in electrochemical reactions. *Electrochimica Acta* **2003**, *49*, 147–152, doi:10.1016/j.electacta.2003.04.009.
4. Fahidy, T. Z. Characteristics of surfaces produced via magnetoelectrolytic deposition. *Prog. Surf. Sci.* **2001**, *68*, 155–188, doi:10.1016/S0079-6816(01)00006-5.
5. Naaman, R.; Waldeck, D. H. Chiral-induced spin selectivity effect. *J. Phys. Chem. Lett.* **2012**, *3*, 2178–2187, doi:10.1021/jz300793y.
6. Kumar, A.; Capua, E.; Kesharwani, M. K.; Martin, J. M. L.; Sitbon, E.; Waldeck, D. H.; Naaman, R. Chirality-induced spin polarization places symmetry constraints on biomolecular interactions. *Proc. Natl. Acad. Sci. U. S. A.* **2017**, *114*, 2474–2478, doi:10.1073/pnas.1611467114.
7. Shi, X.; Wang, Y.; Peng, C.; Zhang, Z.; Chen, J.; Zhou, X.; Jiang, H. Enantiorecognition of Tyrosine Based on a Novel Magnetic Electrochemical Chiral Sensor. *Electrochimica Acta* **2017**, *241*, 386–394, doi:10.1016/j.electacta.2017.04.155.
8. Giancoli, D. C. *Physics for scientists and engineers*; Pearson Education International, 2008;
9. Monzon, L. M. A.; Coey, J. M. D. Magnetic fields in electrochemistry: The Lorentz force. A mini-review. *Electrochem. Commun.* **2014**, *42*, 38–41, doi:10.1016/j.elecom.2014.02.006.
10. Cardona, M.; Peter, Y. Y. *Fundamentals of semiconductors*; Springer, 2005;
11. Alfvén, H. Existence of electromagnetic-hydrodynamic waves. *Nature* **1942**, *150*, 405.
12. Chopart, J.; Olivier, A.; Merienne, E.; Amblard, J.; Aaboubi, O. A New Experimental Device for Convective Mass-Transport Analysis by Electrokinetic-Hydrodynamic Effect. **1998**, *1*, 139–141.
13. Szcześ, A.; Chibowski, E.; Hołysz, L.; Rafalski, P. Effects of static magnetic field on water at kinetic condition. *Chem. Eng. Process. Process Intensif.* **2011**, *50*, 124–127, doi:10.1016/j.cep.2010.12.005.
14. Coey, J. M. D.; Cass, S. Magnetic water treatment. *J. Magn. Magn. Mater.* **2000**, *209*, 71–74, doi:10.1016/S0304-8853(99)00648-4.
15. Kovarsky, R.; Golodnitsky, D.; Peled, E.; Khatun, S.; Stallworth, P. E.; Greenbaum, S.; Greenbaum, A. Conductivity enhancement induced by casting of polymer electrolytes under a magnetic field. *Electrochimica Acta* **2011**, *57*, 27–35, doi:10.1016/j.electacta.2011.04.016.
16. Oliver, A. Tronel-peyroz, a. oliver,. **1980**, *25*, 1–6.
17. Aaboubi, O. Magnetic Field Effects on Mass Transport. *J. Electrochem. Soc.* **1990**, *137*, 1796, doi:10.1149/1.2086807.
18. Aogaki, R.; Fueki, K. Application of a Magnetohydrodynamic Generator-Detector Electrode to Hydrodynamic Voltammetry. *J Electrochem Soc* **1984**, *131*, 1295–1300, doi:10.1149/1.2115809.
19. Rhen, F. M. F.; Coey, J. M. D. Magnetic field effect on autocatalysis: Ag and Cu in concentrated nitric acid. *J. Phys. Chem. B* **2006**, *110*, 6274–6278, doi:10.1021/jp057585+.

20. Chopart, J. P.; Douglade, J.; Fricoteaux, P.; Olivier, A. Electrodeposition and electrodissolution of copper with a magnetic field: dynamic and stationary investigations. *Electrochimica Acta* **1991**, *36*, 459–463, doi:10.1016/0013-4686(91)85128-T.
21. Devos, O.; Aaboubi, O.; Chopart, J.-P.; Olivier, A.; Gabrielli, C.; Tribollet, B. Is There a Magnetic Field Effect on Electrochemical Kinetics? *J. Phys. Chem. A* **2000**, *104*, 1544–1548, doi:10.1021/jp993696v.
22. Aogaki, R.; Negishi, T.; Yamato, M.; Ito, E.; Mogi, I. Hysteresis effect of magnetic field on electron transfer processes in electrochemical reaction. *Phys. B Condens. Matter* **1994**, *201*, 611–615, doi:10.1016/0921-4526(94)91172-X.
23. Kaptein, R. Simple rules for chemically induced dynamic nuclear polarization. *J. Chem. Soc. Chem. Commun.* **1971**, 732, doi:10.1039/c29710000732.
24. Mogi, I.; Morimoto, R.; Aogaki, R.; Watanabe, K. Surface chirality induced by rotational electrodeposition in magnetic fields. *Sci. Rep.* **2013**, *3*, doi:10.1038/srep02574.
25. Mhíocháin, T. R. N.; Coey, J. M. D. Chirality of electrodeposits grown in a magnetic field. *Phys. Rev. E - Stat. Phys. Plasmas Fluids Relat. Interdiscip. Top.* **2004**, *69*, 10, doi:10.1103/PhysRevE.69.061404.
26. Ispas, A.; Matsushima, H.; Plieth, W.; Bund, A. Influence of a magnetic field on the electrodeposition of nickel-iron alloys. *Electrochimica Acta* **2007**, *52*, 2785–2795, doi:10.1016/j.electacta.2006.10.064.
27. Koza, J. A.; Uhlemann, M.; Gebert, A.; Mickel, C.; Baunack, S.; Schultz, L. The effect of magnetic fields on the electrodeposition of CoFe alloys. *Magnetohydrodynamics* **2009**, *53*, 259–266, doi:10.1016/j.electacta.2008.02.082.
28. Mogi, I.; Watanabe, K. Electrocatalytic chirality on magneto-electropolymerized polyaniline electrodes. *J. Solid State Electrochem.* **2007**, *11*, 751–756, doi:10.1007/s10008-006-0191-2.
29. Horvath, J. D.; Koritnik, A.; Kamakoti, P.; Sholl, D. S.; Gellman, A. J. Enantioselective separation on a naturally chiral surface. *J. Am. Chem. Soc.* **2004**, *126*, 14988–14994, doi:10.1021/ja045537h.
30. Ortega Lorenzo, M.; Baddeley, C. J.; Muryn, C.; Raval, R. Extended surface chirality from supramolecular assemblies of adsorbed chiral molecules. *Nature* **2000**, *404*, 376–379, doi:10.1038/35006031.
31. Horvath, J. D.; Gellman, A. J. Enantiospecific desorption of chiral compounds from chiral Cu(643) and achiral Cu(111) surfaces. *J. Am. Chem. Soc.* **2002**, *124*, 2384–2392, doi:10.1021/ja012182i.
32. Duyne, V. Letters To Nature. *October* **2003**, *425*, 3–6, doi:10.1038/nature02020.1.
33. Xie, Y.; Huber, C. Electrocatalysis and Amperometric Detection Using an Electrode Made of Copper Oxide and Carbon Paste Youqin. *Anal. Chem.* **1991**, 1714–1719, doi:10.1021/ac00017a012.
34. Hinds, G.; Spada, F. E.; Coey, J. M. D.; Mhiochain, T. R. N.; Lyons, M. E. G. Magnetic field effects on copper electrolysis. *J.Phys.Chem.B* **2001**, *105*, 9487–9502.
35. Yutthalekha, T.; Wattanakit, C.; Lapeyre, V.; Nokbin, S.; Warakulwit, C.; Limtrakul, J.; Kuhn, A. Asymmetric synthesis using chiral-encoded metal. *Nat. Commun.* **2016**, *7*, 1–8, doi:10.1038/ncomms12678.
36. Frank, R. L.; Hoffman, J. G. Hall Voltage in Electrolyte Solutions. *Phys. Chem. Liq.* **1972**, *3*, 191–204, doi:10.1080/00319107208084099.

37. Hubbard, J. B.; Wolynes, P. G. An electrohydrodynamic contribution to the Hall effect in electrolyte solutions. *J. Chem. Phys.* **1981**, *75*, 3051–3054, doi:10.1063/1.442400.
38. Newman, D. S.; Frank, C.; Matlack, R. W.; Twining, S.; Krishnan, V. The ionic hall effect in the solid electrolyte C5H6NAg5I6. *Electrochimica Acta* **1977**, *22*, 811–814, doi:10.1016/0013-4686(77)80001-7.
39. Wright, J. J. The Hall Effect in a Flowing Electrolyte. *Am. J. Phys.* **1972**, *40*, 245, doi:10.1119/1.1986499.
40. Hall, E. H. On a New Action of the JIa19flet onz Electric. *Am. J. Math.* **2014**, *2*, 287–292.
41. Eckshtain-Levi, M.; Capua, E.; Refaely-Abramson, S.; Sarkar, S.; Gavrilov, Y.; Mathew, S. P.; Paltiel, Y.; Levy, Y.; Kronik, L.; Naaman, R. Cold denaturation induces inversion of dipole and spin transfer in chiral peptide monolayers. *Nat. Commun.* **2016**, *7*, 10744, doi:10.1038/ncomms10744.
42. Kumar, A.; Capua, E.; Vankayala, K.; Fontanesi, C.; Naaman, R. Magnetless Device for Conducting Three-Dimensional Spin-Specific Electrochemistry. *Angew. Chem.* **2017**, *129*, 14779–14782, doi:10.1002/ange.201708829.
43. Walsh, D. A.; Lovelock, K. R. J.; Licence, P. Ultramicroelectrode voltammetry and scanning electrochemical microscopy in room-temperature ionic liquid electrolytes. *Chem. Soc. Rev.* **2010**, *39*, 4185, doi:10.1039/b822846a.
44. Mondal, P. C.; Fontanesi, C.; Waldeck, D. H.; Naaman, R. Spin-dependent transport through chiral molecules studied by spin-dependent electrochemistry. *Acc. Chem. Res.* **2016**, *49*, 2560–2568.
45. Fontanesi, C.; Tassinari, F.; Parenti, F.; Cohen, H.; Mondal, P. C.; Kiran, V.; Giglia, A.; Pasquali, L.; Naaman, R. New one-step thiol functionalization procedure for Ni by self-assembled monolayers. *Langmuir* **2015**, *31*, 3546–3552.
46. Mondal, P. C.; Kantor-Uriel, N.; Mathew, S. P.; Tassinari, F.; Fontanesi, C.; Naaman, R. Chiral Conductive Polymers as Spin Filters. *Adv. Mater.* **2015**, *27*, 1924–1927, doi:10.1002/adma.201405249.
47. Mondal, P. C.; Fontanesi, C.; Waldeck, D. H.; Naaman, R. Field and chirality effects on electrochemical charge transfer rates: spin dependent electrochemistry. *ACS Nano* **2015**, *9*, 3377–3384.